Conformal Double Exponentially Tapered Slot Antenna (DETSA) on LCP for UWB Applications

Symeon Nikolaou, *Student Member, IEEE*, George E. Ponchak, *Senior Member, IEEE*, John Papapolymerou, *Senior Member, IEEE*, and Manos M. Tentzeris, *Senior Member, IEEE*

***Abstract*—We discuss the use of a double exponentially tapered slot antenna (DETSA) fabricated on flexible liquid crystal polymer (LCP) as a candidate for ultrawideband (UWB) communications systems. The features of the antenna and the effect of the antenna on a transmitted pulse are investigated. Return loss and E and H plane radiation pattern measurements are presented in several frequencies covering the whole ultra wide band. The return loss remains below -10 dB and the shape of the radiation pattern remains fairly constant in the whole UWB range (3.1–10.6 GHz). The main lobe characteristic of the radiation pattern remains stable even when the antenna is significantly conformed. The major effect of the conformation is an increase in the cross polarization component amplitude. The system: transmitter DETSA—channel - receiver DETSA is measured in frequency domain and shows that the antenna adds very little distortion on a transmitted pulse. The distortion remains small even when both transmitter and receiver antennas are folded, although it increases slightly.**

***Index Terms*—Conformal antenna, distortion, double exponentially slot antenna (DETSA), liquid crystal polymer (LCP), ultrawideband (UWB), ultrashort pulse.**

I. Introduction

THE rapid developments in broadband wireless communications and the great number of commercial and military applications necessitate new types of antennas which can support higher bit rates. The ultrawideband (UWB) [1] protocol using the spectrum from 3.1 to 10.6 GHz is a new promising technology suitable for high rate communications in small distances. The double exponentially tapered slot antenna (DETSA), which is a variation of the Vivaldi antenna with the outer edge exponentially tapered, was introduced for the first time in [2] with design and performance characteristics discussed in [3] and [4] as a possible UWB antenna. A coplanar waveguide–fed version of DETSA is explored in [5] for a UWB sub-band, while in [6] a Vivaldi antenna is proposed for the ultra wide band. The effect of dielectric substrate and antenna dimensions on the input impedance and the radiation beamwidth on tapered slot antennas is explicitly presented in [7] while a theoretical estimation of the far field radiation pattern that agrees well with measurements is presented in [8].

Manuscript received July 27, 2005; revised November 9, 2005. This work was partially supported by the Georgia Electronic Design Center and partially by the U.S. Army Research Office.

S. Nikolaou, J. Papapolymerou and M. M. Tentzeris are with the Georgia Institute of Technology, Atlanta, GA 30302 USA (e-mail: simos@ece.gatech.edu).

G. E. Ponchak is with NASA Glenn Research Center, Cleveland, OH 44135 USA.

Digital Object Identifier 10.1109/TAP.2006.875915

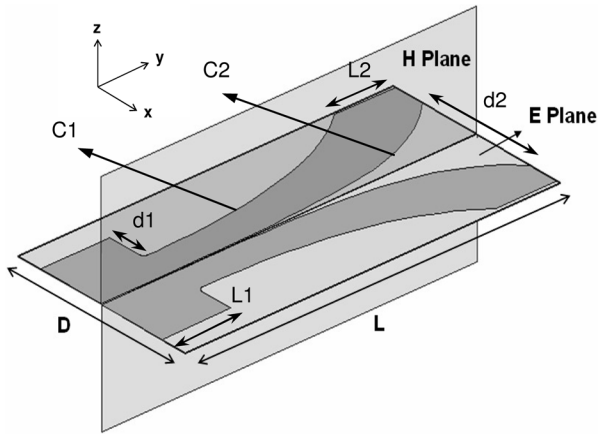

Fig. 1. DETSA schematic E and H planes are defined.

In this paper, a double exponentially tapered slot antenna (DETSA) on flexible LCP organic material suitable for packaging and integration with other components is introduced and proposed for the UWB range with gain above 7 dBi and return loss below -10 dB for the whole frequency range. The antenna is characterized not only in the traditional planar form, but also in the case that is flexed in a conformal shape that mimics the shape of an automobile hood or bumper or the leading edge of an aircraft wing, and the characteristics of the two antenna shapes are compared. Lastly, we use a frequency domain measurement to estimate the distortion in data pulses caused by the DETSA, which varies from the time domain measurements in [9], [10].

II. Antenna Design

The proposed antenna was fabricated on a 200 μm thick liquid crystal polymer (LCP) substrate with an 18 μm thick copper layer. The DETSA schematic is presented in Fig. 1. The length of the board is $L = 13.62$ cm, the width is $D = 6.64$ cm, and the slot gap at the feeding point is 100 μm wide. LCP was preferred because of a number of desirable features.

The dielectric constant $\varepsilon_r = 3.1$ is low enough to be used for an end-fire antenna, it has low loss $(\tan\delta = 0.002)$ while being conformal, and it is easy to fabricate with an engineered coefficient of thermal expansion (CTE) [11]. Standard photolithography was used for the fabrication. The design dimensions have been optimized for the antenna to be matched over a frequency range of 3 to 11 GHz. The design parameters are summarized in Table I. For contours C1 and C2, y variable starts at distance L1 from the edge of the board and it is measured in centimeters.

TABLE I
DIMENSIONS OF DETSA

C1	0.76exp(0.16y) 0<y<8.53 cm
C2	0.012exp(0.48y) 0<y<10.67 cm
d1	12.00 mm
d2	42.92 mm
L1	24.00 mm
L2	21.40mm
D	66.40 mm
L	130.70 mm

III. RETURN LOSS AND RADIATION PATTERN MEASUREMENTS

A. Return Loss Measurement

For return loss and radiation pattern measurements, an SMA connector was soldered directly on the slot with no tuning components. The antenna was folded in such a way that the end of the board forms an 18° angle with y axis as shown in Fig. 4. The contour that describes the projection of the resulted folded antenna surface on the H plane is given by (1) where the y variable is measured in centimeters and starts at the origin as shown in Fig. 4

$$C(y) = -0.0126(y+1.451y^2+0.074y^3) \qquad 0 \le y \le 10.67\ \text{cm}. \quad (1)$$

Ansoft HFSS 9.0 software [12] was used for the full wave simulations. The simulated and measured return loss is presented in Fig. 2, where it can be seen that good agreement is achieved between simulated and measured return loss, that there is no difference between flat and folded, conformal, antenna return loss, and the return loss remains below -10 dB in the whole UWB range. The observed "saw" pattern instead of a resonance dominated pattern is expected because the DETSA is a traveling wave antenna with a non-matched termination, not a resonance radiation element. The measured return loss is in agreement with the results in [13]. For the frequencies in the 8 to 10.6 GHz range the return loss is below -15 dB. In those frequencies relatively higher gain is measured. The planar and folded antennas are shown in Fig. 3(a) and (b), respectively.

B. Radiation Pattern Measurements

For the radiation pattern diagrams both near and far field measurements were taken. For all of the measurements, the DETSA is placed between two pieces of 1.5 cm thick styrofoam to give the antenna mechanical support. The styrofoam is cut into the same shape as the DETSA for the conformal antenna. The contour that describes the conformal antenna is a projection on the H plane that is given by (1). During characterization of the conformal antenna, the $x-z$ plane at $y=0$ is located at the SMA connector and the y axis is along the direction of the SMA adapter. Thus, while E and H plane cut definitions are not changed in the presentation of the results, the DETSA antenna is not in the $x-y$ plane as shown in Fig. 1. In fact, if a straight line approximation to the conformal antenna is used, the antenna is pointing downward at an angle of 18° to the y axis as shown in Fig. 4. Despite the unbalanced feeding, the agreement between the balanced excited simulation and the (unbalanced) measurement is good as can be seen in Fig. 5, indicating that the unbalanced feeding does not have any major effect on the radiation patterns.

For the near field measurements, a cylindrical range from Nearfield Systems Inc. is used with an HP8530A microwave receiver. To cover the frequency range of 3 to 12 GHz, four probes,

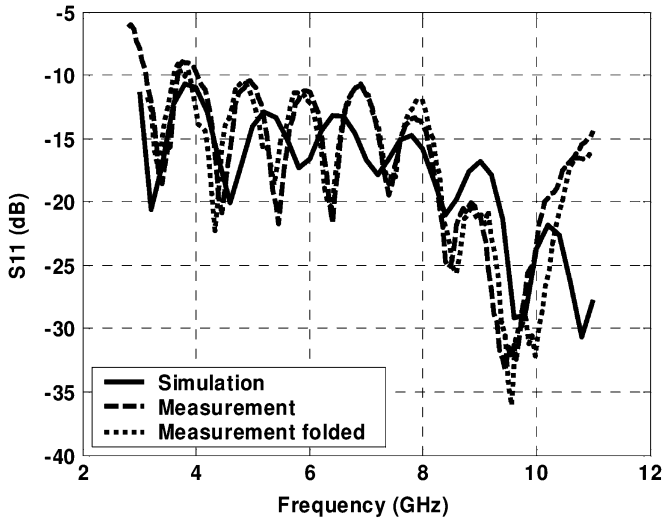

Fig. 2. Return loss simulation and measurement for planar and folded antenna.

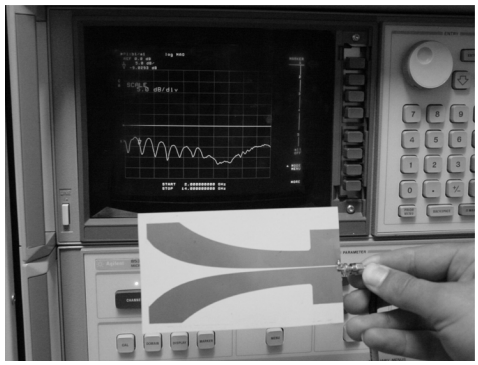

(a)

(b)

Fig. 3. (a) Planar DETSA antenna and (b) folded DETSA antenna connected to the HP 8530A Network Analyzer.

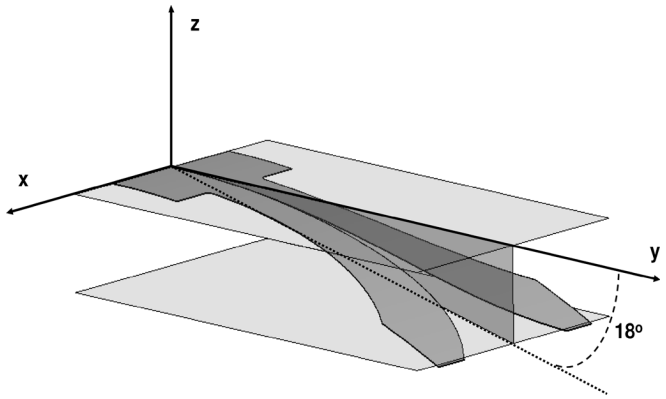

Fig. 4. Folded DETSA schematic. The antenna is pointing downward at an angle of 18° to the y axis.

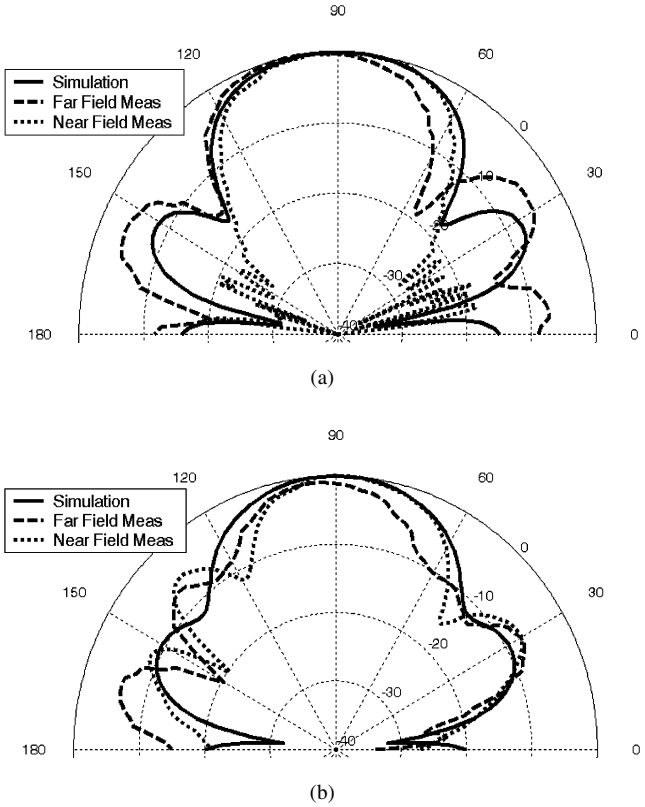

Fig. 5. (a) E plane and (b) H plane simulation far and near field measurement $f = 5$ GHz.

one for each waveguide band, are used. The measured near field magnitude and phase are transferred to the far field with a 2-D Fourier transform performed by the near field range software. The maximum scan in the vertical direction is 110 cm, which reduces the accuracy of the system as configured for measuring the DETSA for radiation patterns at angles greater than 62° off axis.

The main problem with wideband antennas is the electrical length variation with frequency, which causes significant distortion in the radiation patterns. Generally, an increase in frequency in end-fire antennas causes the main beam to become narrower (reduced beamwidth) and the directivity to increase. The y axis in Fig. 1 corresponds to $\phi = 90°$ for the E plane cuts and to

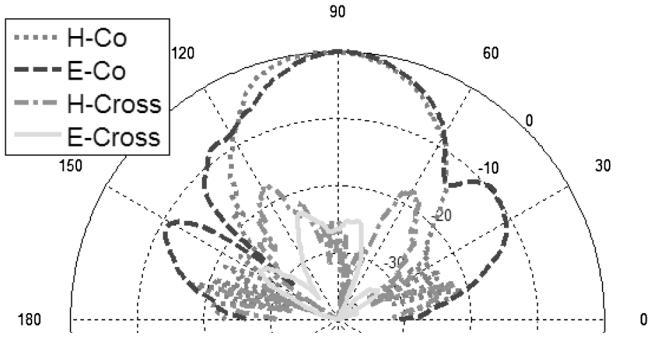

Fig. 6. Planar DETSA $f = 6$ GHz.

$\theta = 90°$ for the H plane cuts. The x axis corresponds to $\phi = 0°$ and z axis to $\theta = 0°$. E and H planes with respect to the antenna and axes orientation can be seen in Fig. 1.

In Fig. 5, the far and near field measurements are presented at 5 GHz with the simulated radiation patterns for the planar antenna. There is very good agreement between the measured field patterns from the near and far field ranges except for the E plane near field pattern for angles greater than 60° off axis. This limit in the near field measurements was already discussed. Furthermore, there is excellent agreement between the simulated and far field radiation patterns except for small errors in the magnitude of the side lobes.

The wideband behavior of the planar DETSA is shown in Figs. 6–8 where radiation pattern measurements are presented. The radiation pattern is similar from 4 to 10 GHz. It is also seen that the cross-polarization cuts, labeled H-cross and E-cross, are below -15 dB across the frequency band and below -20 dB at some frequencies. There is a slight asymmetry in the sidelobes, especially noticeable in the E co-cuts; we believe this is due to the SMA launcher and coaxial cable that was positioned below the antenna or at angles greater than 90°. The asymmetry in the planar antennas is constant with respect to frequency. This overall radiation pattern consistency over a wide frequency band is the major advantage of the DETSA, especially with respect to competitive UWB designs [14], [15]. However, the measured gain varies with respect to frequency as shown in Table II that demonstrates that the gain increases linearly with frequency.

The applicability of a DETSA fabricated on a very thin, flexible substrate for conformal antennas is also shown in Fig. 7. By comparing the planar to the folded DETSA radiation patterns, it is seen that the E co-pattern is nearly identical. As expected, the H co-pattern is pointed towards $\theta > 90°$ [downward with respect to the y axis as per (1)], due to the folding of the antenna in the H-plane. Furthermore, the pattern is skewed more as frequency increases, and for 10 GHz, the beam points 18° off axis as predicted by the shape of the folded DETSA. There is an increase in the cross-polarization level for the folded DETSA, especially in E-cross and in the direction of the H co-pattern, which agrees with the observations of Lee and Simons for folded tapered slot antennas [16] and [17]. Generally though, the shape of the beam does not vary with folding. This can be verified with an inspection of Fig. 8 where 3-D patterns are presented. The off-axis field magnitude for the planar antenna is below -20 dB, and it is below -10 dB for the folded antenna for the main

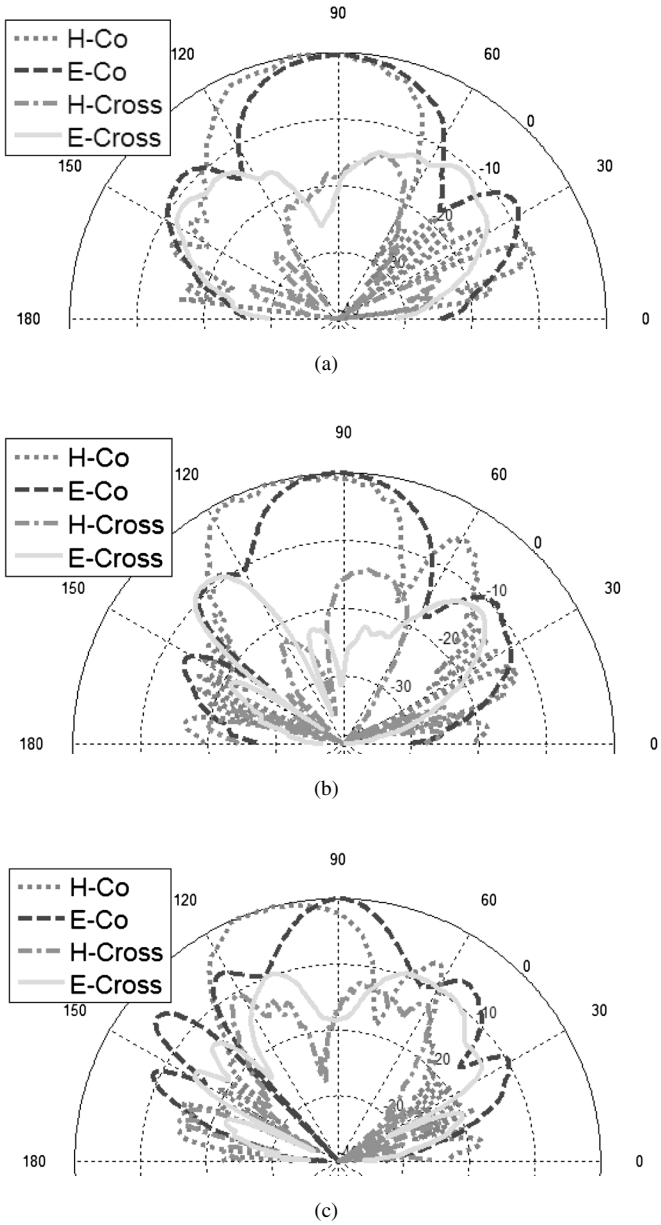

Fig. 7. Folded DETSA (a) $f = 4$ GHz, (b) $f = 6$ GHz, and (c) $f = 10$ GHz.

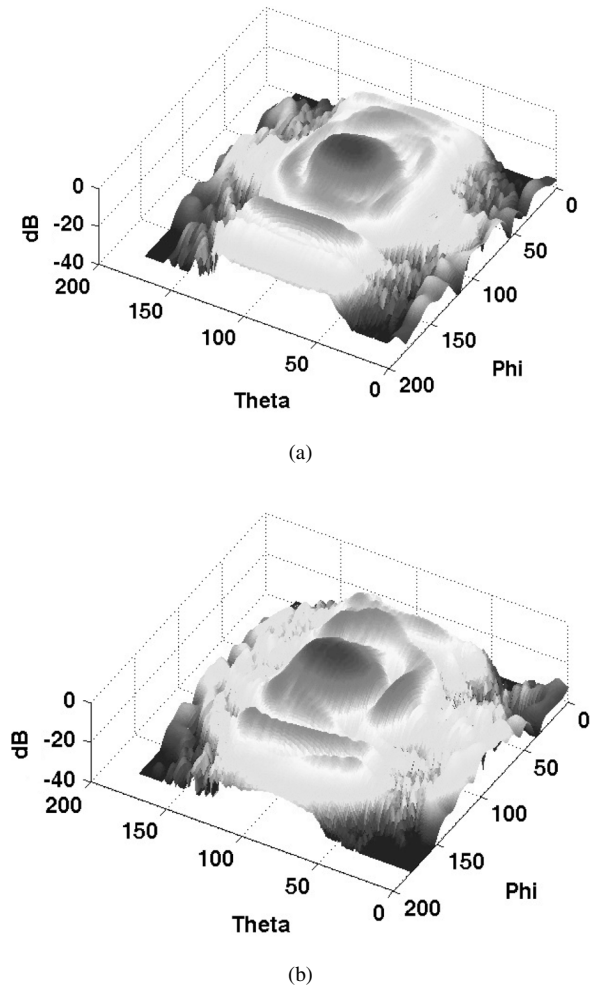

Fig. 8. (a) Planar and (b) folded DETSA 3-D pattern $f = 8$ GHz.

TABLE II
MEASURED GAIN OF PLANAR DETSA

Frequency [GHz]	Gain [dBi]
3	7.4
4	7.8
5	7.0
6	9.8
8	11.9
10	10.6

beam. This 10 dB increase in off-axis field magnitude and the maximum gain direction which is directed at $\theta = 108°$ are the major effects caused by folding.

IV. Frequency Domain Measurement for Distortion Estimation

A. Setup

To get an estimate of the effect of the antenna on a transmitted pulse, the setup in Fig. 9 was used. Two antennas are used, one as a transmitter and the second as a receiver. The two DETSA antennas are aligned with the SMA launcher or y-axis of each antenna pointing at each other and the distance between them is set at 1.5 m. The minimum far field distance given from $\mathrm{R} = 2D^2/\lambda$ is calculated at 0.65 m when $D = 13.6$ cm and λ for 10.6 GHz are used. Both antennas are connected to an HP 8530A network analyzer and S_{21} measurement is taken. The antennas' planes are kept perpendicular to the ground as they appear in Fig. 3 to avoid the use of mechanical support with styrofoam. The measurement is repeated when both the antennas are identically conformed and the SMA launcher of each still aligned. The whole process takes place in a laboratory environment that resembles an actual communications environment more realistically compared to a potential measurement in an anechoic chamber. The measurements are presented in Fig. 10 for both planar and folded antennas. The misalignment, as a result of the folding, causes higher fading for the higher frequencies (8–10.6 GHz) due to the respective higher directivity and

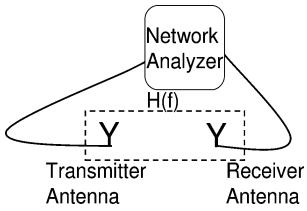

Fig. 9. Setup for the system: transmitter - channel - receiver, frequency domain measurement.

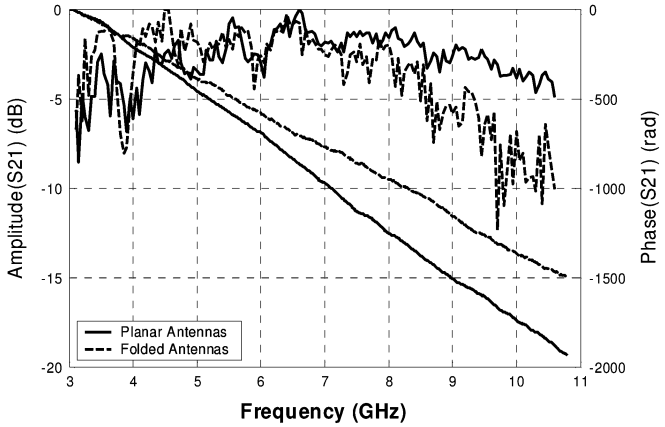

Fig. 10. S_{21} measurements for the system: transmitter - channel - receiver.

the increasing skew in the radiation pattern with frequency as seen in Fig. 7. The phase however in both cases remains linear.

B. Distortion Estimation

The S_{21} measurement represents the transfer function H(f) of a "black box" that consists of the transmitter DETSA the 1.5 m laboratory environment channel and the receiver DETSA. Any time domain pulse s(t) to be transmitted has a Fourier transform S(f). The pulse detected at the receiver has a Fourier transform $\mathrm{R(f)} = \mathrm{S(f)H(f)}$. The transmitted pulse s(t) and the received pulse $\mathrm{r(t)} = \mathrm{F^{-1}\{R(f)\}}$ are correlated to get an estimation of the distortion added by the DETSA UWB communications system. The distance between the two antennas is long enough to guarantee a far field measurement and at the same time, small enough that it is reasonable to assume that the distortion is caused mainly by the antennas and not by the wireless channel itself. We investigate the effect on an ideal rectangular pulse of duration of 1 ns. The spectrum for a rectangular pulse is mainly concentrated around the dc frequency and goes to zero at n/To where To is the pulse duration that equals to 1 ns, and $\mathrm{n} \in \mathrm{N}$. We compare the received pulse with the equivalent time domain

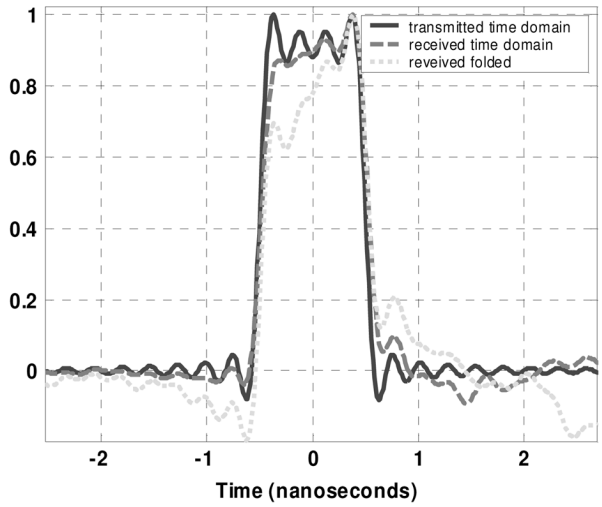

Fig. 11. Time domain rectangular pulse The solid line pulse is a rectangular pulse with 7.5 (10.6-3.1) GHz bandwidth that is used as a transmitted pulse. The duration of the pulse is only 1 ns. Small distortion is added by the system: transmitter - channel - receiver.

pulse that is created when the rectangular pulse baseband spectrum is modulated at $(6.85 = (10.6{+}3.1)/2)$ GHz and filtered from an ideal passband filter with passband range at 3.1–10.6 GHz. The superimposed pulses are presented in Fig. 11 and very good agreement is observed. The folded antennas cause stronger distortion than the planer antennas but still the maximum correlation value, estimated with function (2), results in 0.96 for the folded antennas and 0.99 for the planar antennas

$$\mathrm{Corr}(d) = \frac{\sum_i \left[(x(i) - m_x)\left(y(i-d) - m_y\right)\right]}{\sqrt{\sum_i (x(i) - m_x)^2}\sqrt{\sum_i (y(i) - m_y)^2}} \tag{2}$$

$x(i)$ and $y(i)$ are the compared waveforms, m_x and m_y are the respected mean values.

The rectangular pulse is an ideal pulse and is not used in practice for any communication systems because of the huge spectrum required. Therefore we use a raised cosine pulse to investigate the same effect. The raised cosine pulse has a spectrum (3) that causes zero intersymbol interference (ISI) and is a popular pulse for several modulations. The time domain pulse as a result of the spectrum described by (3) is given by (4), shown at the bottom of the page.

For the pulse presented in Fig. 12 $Ts = 1/BW$ was used, where $BW = (10.6\text{–}3.1)$ GHz and the roll-off factor is $\alpha = 0.5$. The pulse described from the analytical expression (4) is plotted with the normalized inverse Fourier transform of the pulse's spectrum multiplied by the measured H(f) and very good

$$H_{\mathrm{rc}} = \begin{cases} Ts & 0 \le |f| \le (1-a)/2Ts \\ \frac{Ts}{2}\left[1 - \sin\frac{\pi Ts}{a}\left(|f| - \frac{Ts}{2}\right)\right] & (1-a)/2Ts \le |f| \le (1+a)/2Ts \\ 0 & (1+a)/2Ts \le |f| \end{cases} \tag{3}$$

$$s_{\mathrm{RC}} = F^{-1}\{H_{\mathrm{RC}}(f)\} = \frac{\sin(\pi t/\mathrm{Ts})}{\pi t/\mathrm{Ts}} \frac{\cos(a\pi t/Ts)}{1 - 4a^2t^2/Ts^2}. \tag{4}$$

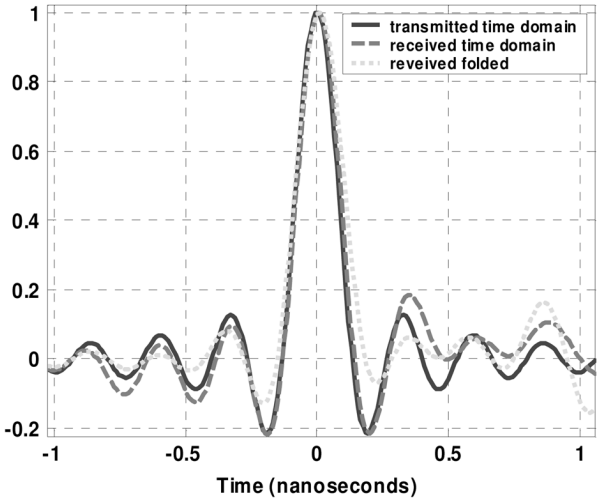

Fig. 12. Time domain pulse described by (4) superimposed with distorted pulse from both planar and folded antennas. The pulse has theoretically infinite duration because of the confined spectrum but it decays with 1/t.

agreement is deduced (Fig. 11). The maximum correlation value is estimated at 0.98 for the planar antennas and 0.95 for the folded antennas.

The measurement and the mathematical analysis of the data clearly indicate that very little distortion is introduced by the antennas, and the antennas practically do not affect in a destructive way the transmitted pulses. This is mainly due to their broadband performance (3.1–10.6 GHz) and high directivity.

V. Conclusion

A DETSA on flexible organic material (LCP), suitable for conformal packaging and integration with other components, is introduced and proposed for the UWB range. The measurements agree fairly well with the simulations and this antenna is proved to perform well in the whole UWB range. Return loss below -10 dB is measured for the whole frequency range of operation both when the antenna remains planar and when is folded. The antenna performs with high gain starting from 7 dBi for low frequencies and up to 12 dBi for the higher frequencies. Near and far field measurements in several frequencies covering the whole UWB band indicate that the radiation pattern remains fairly constant and within the specifications for a UWB communications system. Frequency domain measurements indicate that the antenna, when is planar or even when is significantly folded causes minimum distortion to any transmitted pulse. The antenna on LCP is conformal, can be easily fabricated with relatively low cost and is a good candidate for a number of UWB applications.

References

[1] M. Z. Win and R. A. Scholtz, "Ultra-wide bandwidth (UWB) time-hopping spread-spectrum impulse radio for wireless multiple access communications," in *IEEE Trans. Commun.*, Apr. 2000, vol. 48, no. 4, pp. 679–689.

[2] J. J. Lee and S. Livingston, "Wide band bunny-ear radiating element," in *Proc. IEEE Antennas Propagation Soc. Int. Symp.*, Ann Arbor, MI, Jul. 1993, pp. 1604–1607.

[3] M.C. Greenberg and L.L. Virga, "Characterization and design methodology for the dual exponentially tapered slot antenna," in *Proc. IEEE Antennas and Propagation Soc. Int. Symp.*, Atlanta, GA, Jul. 1999, vol. 1, pp. 88–91.

[4] M.C. Greenberg, K.L. Virga, and C.L. Hammond, "Performance characteristics of the dual exponentially tapered slot antenna (DETSA) for wireless communications applications," *IEEE Trans. Veh. Technol.*, vol. 52, no. 2, pp. 305–312, Mar. 2003.

[5] Yo-Shen Lin, Tzyh-Ghuang Ma, Shyh-Kang Jeng, and Chun Hsiung Chen, "Coplanar waveguide-fed dual exponentially tapered slot antennas for ultra-wideband applications," in *Proc. Antennas and Propagation Soc. Symp.*, Monterey, CA, Jun. 2004, vol. 3, pp. 2951–2954.

[6] Sang-Gyu Kim and K. Chang, "Ultra wideband exponentially-tapered antipodal Vivaldi antennas," in *Proc. IEEE Antennas and Propagation Soc. Symp.*, Monterey, CA, Jun. 2004, vol. 3, pp. 2273–2276.

[7] K. S. Yngvesson, D. H. Schaubert, T. L. Korzeniowski, E. L. Kollberg, T. Thungren, and J. F. Johansson, "Endfire tapered slot antennas on dielectric substrates," *IEEE Trans. Antennas Propag.*, vol. AP-33, pp. 1392–1400, Dec. 1985.

[8] Janaswamy and D. H Schaubert, "Analysis of the tapered slot antenna," *IEEE Trans. Antennas Propag.*, vol. AP-35, pp. 1058–1064, Sep. 1987.

[9] J. Powell and A. P. Chandrakasan, "Spiral slot patch antenna and circuilar disc monopole for ultra wideband communication," presented at the Int. Symp. Antennas and Propagation, Aug. 2004.

[10] J. Powell and A. P. Chandrakasan, "Differential and single ended elliptical antennas for 3.1–10.6 GHz ultra wideband communication," presented at the Proc. IEEE Antennas and Propagation Soc. Symp., Monterey, CA, Jun. 2004.

[11] D.C. Thompson, O. Tantot, H. Jallageas, G.E. Ponchak, M.M. Tentzeris, and J. Papapolymerou, "Characterization of liquid crystal polymer (LCP) material and transmission lines on LCP substrates from 30 to 110 GHz," *IEEE Trans. Microw. Theory Tech.*, vol. 52, no. 4, pp. 1343–1352, Apr. 2004.

[12] *Ansoft HFSS 9.0 User manual*, San Jose, CA.

[13] J.D.S. Langley, P.S. Hall, and P. Newham, "Balanced antipodal Vivaldi antenna for wide bandwidth phased arrays," *Proc. Inst. Elect. Eng. Microwaves Antennas and Propagation*, vol. 143, no. 2, pp. 97–102, Apr. 1996.

[14] Hyungkuk Yoon, Hyungrak Kim, Kihun Chang, Young Joong Yoon, and Young-Hwan Kim, "A study on the UWB antenna with band-rejection characteristic," in *Proc. IEEE Antennas and Propagation Soc. Symp.*, Monterey, CA, Jun. 2004, vol. 2, pp. 1784–1787.

[15] Tzyh-Ghuang Ma and Shyh-Kang Jeng, "A compact tapered-slot-feed annular slot antenna for ultra-wideband applications," in *Proc. IEEE Antennas and Propagation Soc. Symp.*, Monterey, CA, Jun. 2004, vol. 3, pp. 2943–2946.

[16] R. Q. Lee and R. N. Simons, "Effect of curvature on tapered slot antennas," in *Proc. IEEE Antennas and Propagation Soc. Symp.*, Jul. 1996, vol. 1, pp. 188–191.

[17] K. F. Lee and W. Chen, *Advances in Microstrip and Printed Antennas*. New York: Wiley, 1997, pp. 477–479.

Symeon Nikolaou (S'06) received the Diploma in electrical and computer engineering from the National Technical University of Athens (NTUA), Athens, Greece, in 2003, and the M.S. in electrical and computer engineering from Georgia Institute of Technology, Atlanta, in 2005. He is currently working toward the Ph.D. degree in electrical engineering at the Georgia Institute of Technology, Atlanta.

His current research interests include the design and development of compact UWB and reconfigurable antennas, and RF packaging and design.

George E. Ponchak (S'82–M'83–SM'97) received the B.E.E. degree from Cleveland State University, Cleveland, OH, in 1983, the M.S.E.E. degree from Case Western Reserve University, Cleveland, in 1987, and the Ph.D. in electrical engineering from the University of Michigan, Ann Arbor, in 1997.

He joined the staff of the Communication Technology Division at NASA Glenn Research Center, Cleveland, in 1983 where he is now a Senior Research Engineer. In 1997–1998 and 2000–2001, he was a Visiting Lecturer at Case Western Reserve University. He has authored and coauthored 115 papers in refereed journals and symposia proceedings. His research interests include the development and characterization of microwave and millimeter-wave printed transmission lines and passive circuits, multilayer interconnects, uniplanar circuits, Si and SiC Radio Frequency Integrated Circuits, and microwave packaging.

Dr. Ponchak received the Best Paper Award at the ISHM'97 30th International Symposium on Microelectronics Award. He is a senior member of the IEEE Microwave Theory and Techniques Society (MTT-S), a member of the International Microelectronics and Packaging Society (IMAPS), and an Associate Member of the European Microwave Association. He was the Editor of a special issue of the IEEE TRANSACTIONS ON MICROWAVE THEORY AND TECHNIQUES on Si MMICs. He founded the IEEE Topical Meeting on Silicon Monolithic Integrated Circuits in RF Systems, served as its Chair in 1998, 2001, and 2006, and was its Digest Editor in 2000 and 2003. He founded the Cleveland MTT-S/AP-S Chapter and serves as its Chair. He has chaired many MTT-S International Microwave Symposium workshops and special sessions. He is a member of the IEEE International Microwave Symposium Technical Program Committee on Transmission Line Elements and served as its Chair in 2003-2005. He is a member of the IEEE MTT-S AdCom Membership Services Committee and the IEEE MTT-S Technical Committee 12 on Microwave and Millimeter-Wave Packaging and Manufacturing.

John Papapolymerou (S'90–M'99–SM'04) received the B.S.E.E. degree from the National Technical University of Athens, Athens, Greece, in 1993, and the M.S.E.E. and Ph.D. degrees from the University of Michigan, Ann Arbor, in 1994 and 1999, respectively.

From 1999 to 2001 he was a faculty member at the Department of Electrical and Computer Engineering of the University of Arizona, Tucson and during the summers of 2000 and 2003 he was a Visiting Professor at The University of Limoges, France. From 2001 to 2005, he was an Assistant Professor at the School of Electrical and Computer Engineering of the Georgia Institute of Technology, where he is currently an Associate Professor. He has authored or coauthored over 120 publications in peer reviewed journals and conferences. His research interests include the implementation of micromachining techniques and MEMS devices in microwave, millimeter-wave and THz circuits and the development of both passive and active planar circuits on semiconductor (Si/SiGe, GaAs) and organic substrates (LCP, LTCC) for System-on-a-Chip (SOC)/ System-on-a-Package (SOP) RF front ends.

Dr. Papapolymerou received the 2004 Army Research Office (ARO) Young Investigator Award, the 2002 National Science Foundation (NSF) CAREER award, the Best Paper Award at the 3rd IEEE International Conference on Microwave and Millimeter-Wave Technology (ICMMT2002), Beijing, China and the 1997 Outstanding Graduate Student Instructional Assistant Award presented by the American Society for Engineering Education (ASEE), The University of Michigan Chapter. His student also received the best student paper award at the 2004 IEEE Topical Meeting on Silicon Monolithic Integrated Circuits in RF Systems, Atlanta, GA. He currently serves as the Vice-Chair for Commission D of the U.S. National Committee of URSI and as an Associate Editor for the IEEE TRANSACTIONS ON ANTENNAS AND PROPAGATION. During 2004 he was the Chair of the IEEE MTT/AP Atlanta Chapter.

Manos M. Tentzeris (S'89–M'98–SM'03) received the diploma degree in electrical and computer engineering (*magna cum laude*) from the National Technical University of Athens, Greece, and the M.S. and Ph.D. degrees in electrical engineering and computer science from the University of Michigan, Ann Arbor.

He was a Visiting Professor with the Technical University of Munich, Germany for the summer 2002, where he introduced a course in the area of high-frequency packaging. He is currently an Associate Professor with the School of Electrical and Computer Engineering, Georgia Institute of Technology (Georgia Tech), Atlanta. He has helped develop academic programs in highly integrated/multilayer packaging for RF and wireless applications, microwave MEMs, SOP-integrated antennas and adaptive numerical electromagnetics (FDTD, multiresolution algorithms) and heads the ATHENA research group (15 researchers). He is the Georgia Tech NSF-Packaging Research Center Associate Director for RF Research and the RF Alliance Leader. He is also the leader of the RFID Research Group of the Georgia Electronic Design Center (GEDC) of the State of Georgia. He has given more than 40 invited talks in the same area to various universities and companies in Europe, Asia and America. He has published more than 200 papers in refereed Journals and Conference Proceedings and eight book chapters and he is in the process of writing two books.

Dr. Tentzeris is a member of the International Scientific Radio Union (URSI)-Commission D, an Associate Member of EuMA, and a member of the Technical Chamber of Greece. He was the recipient of the 1997 Best Paper Award of the International Hybrid Microelectronics and Packaging Society for the development of design rules for low-crosstalk finite-ground embedded transmission lines. He received the 2000 NSF CAREER Award for his work on the development of MRTD technique that allows for the system-level simulation of RF integrated modules, the 2001 ACES Conference Best Paper Award, the 2002 International Conference on Microwave and Millimeter-Wave Technology Best Paper Award (Beijing, China) for his work on Compact/SOP-integrated RF components for low-cost high-performance wireless front-ends, the 2002 Georgia Tech-ECE Outstanding Junior Faculty Award, the 2003 NASA Godfrey "Art" Anzic Collaborative Distinguished Publication Award for his activities in the area of finite-ground low-loss low-crosstalk coplanar waveguides, the 2003 IBC International Educator of the Year Award, the 2003 IEEE CPMT Outstanding Young Engineer Award for his work on 3-D multilayer integrated RF modules, and the 2004 IEEE Transactions on Advanced Packaging Commendable Paper Award. He was also the 1999 Technical Program Co-Chair of the 54th ARFTG Conference, Atlanta, GA and he is the Vice-Chair of the RF Technical Committee (TC16) of the IEEE CPMT Society. He has organized various sessions and workshops on RF/Wireless Packaging and Integration in IEEE ECTC, IMS, and APS Symposia in all of which he is a member of the Technical Program Committee in the area of "Components and RF." He is an Associate Editor of the IEEE TRANSACTIONS ON ADVANCED PACKAGING.